DOI 10.24425/aee.2026.7546

A Pareto meta-front approach to the optimization of reconfigurable millimeter-wave passive reflectors

PAOLO DI BARBA [1], **ŁUKASZ JANUSZKIEWICZ** [2]✉

[1] *Department of Electrical, Computer and Biomedical Engineering, University of Pavia*
Via Ferrata 5 – 27100 Pavia, Italy

[2] *Institute of Electronics, Lodz University of Technology*
116 Żeromskiego St., 90-924 Lodz, Poland

e-mail: ✉ *lukasz.januszkiewicz@p.lodz.pl, paolo.dibarba@unipv.it*

(Received: 01.09.2026, revised: 19.10.2026)

Abstract: The paper proposes a Pareto meta-front approach for the multi-objective design of reconfigurable millimeter-wave passive reflectors. For each value of a generalized cost parameter, such as wave frequency, a conventional Pareto front is generated by simultaneously maximizing the Radar Cross Section (RCS) and minimizing the physical surface area of the array. The utopia point is then determined, and the Pareto-optimal solution with the minimum Euclidean distance from it is selected as the best compromise. Repeating this procedure over the parameter range yields the *Pareto meta-front*, defined as the locus in the objective space that tracks the evolution of the preferred trade-off across a family of Pareto fronts indexed by different values of the generalized cost parameter. The solutions associated with points on this curve are referred to as *meta-optimal solutions*. The proposed method is applied to a reconfigurable passive dipole array for intelligent reflecting surface applications. The array employs variable element lengths and switchable reactive loads to control the phase distribution and electronically steer the reflected beam. Array geometry and load values are jointly optimized over the 50–70 GHz frequency range to maximize the RCS while minimizing reflector area and maintaining performance over a broad angular range. In the proposed frequency-indexed formulation, the incident-wave frequency serves as the generalized cost parameter. The resulting meta-front identifies frequency-dependent configurations that provide an effective compromise between reflectivity and physical size, establishing a systematic frequency-indexed multi-objective framework for wideband electromagnetic wave redirection.

Key words: design optimization, electromagnetic analysis, meta-optimal solutions, Pareto optimality, reconfigurable antenna array

© 2026. The Author(s). This is an open-access article distributed under the terms of the Creative Commons Attribution-NonCommercial-NoDerivatives License (CC BY-NC-ND 4.0, https://creativecommons.org/licenses/by-nc-nd/4.0/), which permits use, distribution, and reproduction in any medium, provided that the Article is properly cited, the use is non-commercial, and no modifications or adaptations are made.

1. Introduction

Reflectarray antennas are planar arrays of radiating elements illuminated by a feed antenna. They combine the advantages of conventional reflector antennas and phased arrays by imposing a prescribed phase distribution across the reflecting surface to shape or steer the reflected electromagnetic beam. As a result, reflectarrays can focus or redirect electromagnetic energy similarly to conventional parabolic reflectors, while maintaining a significantly lower profile and offering considerable flexibility in beam shaping and scanning [1]. The phase response of each unit cell can be controlled through its geometry or, in reconfigurable configurations, through electronic tuning, enabling either fixed or dynamically reconfigurable radiation patterns. Reflectarrays have consequently been investigated for a wide range of applications, including broadband operation, multibeam radiation, beam scanning, and emerging reconfigurable electromagnetic systems [1, 2].

In emerging sixth-generation (6G) wireless systems, intelligent and adaptive electromagnetic structures are expected to play an increasingly important role in enabling reliable, high-capacity, and energy-efficient communication links. Intelligent Reflecting Surfaces (IRSs), also referred to as Reconfigurable Intelligent Surfaces (RISs), have attracted considerable attention as a means of dynamically modifying the wireless propagation environment by controlling the interaction of electromagnetic waves with a large number of reconfigurable elements [3–5]. By appropriately controlling the phase response of the individual elements, an intelligent reflecting surface can redirect electromagnetic energy toward desired directions and thereby provide a form of programmable passive beamforming. The concept has been extensively investigated in the context of beyond 5G and 6G wireless networks, where intelligent surfaces are considered a potential enabling technology for improving coverage, spectral efficiency, and energy efficiency [3–7]. This concept is shown schematically in Fig. 1.

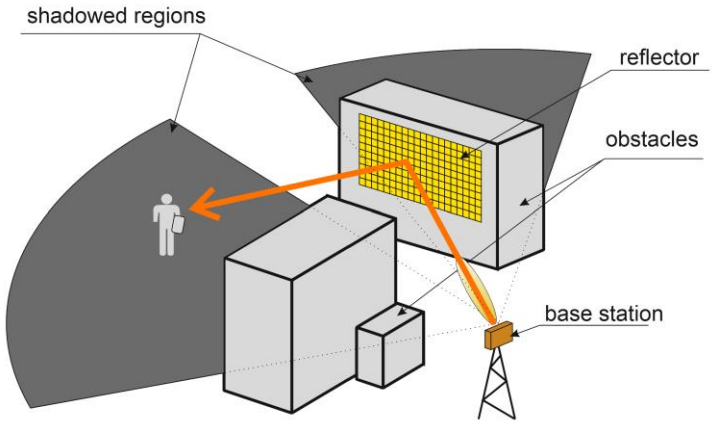


Fig. 1. Reflecting structure applied to 6G system

Although many IRS implementations are based on electronically controlled phase-shifting elements and system-level optimization involving channel estimation, reflectarray architectures provide an alternative electromagnetic implementation in which the required phase distribution

can be directly generated by the radiating elements of the array. In particular, the phase response of individual elements can be modified by connecting suitable reactive loads to their ports. Such an approach can provide a relatively simple mechanism for electronic control of the reflected wave without requiring conventional transmission-line phase shifters. Reactive control of array directivity is an established concept originating in reactively controlled directive arrays [8] and subsequently reviewed for reconfigurable reflectarrays and array lenses [2]. Furthermore, the use of radiating elements designed for multiple operating frequencies can facilitate broadband or multiband operation. These characteristics make reconfigurable reflectarrays attractive candidates for intelligent reflecting structures operating at millimeter-wave frequencies.

The design of such structures, however, involves several competing requirements. The geometrical parameters of the radiating elements and the array, together with the values of the reactive loads, affect the electromagnetic response in a strongly coupled manner. At the same time, high reflectivity must be achieved over a sufficiently broad angular range and frequency band, while the physical dimensions of the array should preferably be limited. The resulting problem is therefore inherently multi-objective and cannot, in general, be reduced to the optimization of a single performance metric without introducing arbitrary weighting among the competing objectives. A single-objective formulation based on weighted objectives may indeed provide a particular compromise, but the resulting solution depends on the selected weighting factors and may not adequately represent the available trade-offs.

Multi-objective optimization provides a natural framework for addressing this type of problem by identifying the set of nondominated solutions, commonly referred to as the Pareto-optimal set, whose corresponding objective vectors form the Pareto front [9, 10]. Since a Pareto front generally contains multiple solutions corresponding to different trade-offs among the objectives, an additional criterion is required when a single representative configuration has to be selected. One possible approach is to define the utopia point in the objective space and identify the Pareto-optimal solution closest to this point according to a suitable distance metric [10, 11]. In the present work, the Euclidean distance is adopted to identify the best-compromise configuration.

The selection of an appropriate optimization strategy is also an important aspect of computational electromagnetics, particularly when electromagnetic performance must be evaluated repeatedly for different design parameters and operating conditions. Comparative studies of nonlinear optimization algorithms, such as the approach presented in [12] in terms of performance, robustness and computational speed, provide additional methodological context for the selection of numerical optimization techniques in electromagnetic design.

In a previous work, the authors introduced the concept of a Pareto meta-front for the optimal design of reconfigurable devices in electromechanics [13]. The concept considers a family of Pareto fronts generated for different values of an external variable parameter. For each parameter value, the corresponding Pareto front is determined, its utopia point is identified, and the Pareto-optimal solution closest to the utopia point is selected as the representative best-compromise solution. The locus connecting these solutions as the external parameter varies defines the Pareto meta-front [13]. Unlike a conventional Pareto front, which describes the trade-offs among competing objectives for a fixed value of the parameter, the Pareto meta-front describes how the best compromise among those objectives evolves across a family of related optimization problems.

The present work extends this concept to computational electromagnetics and, in particular, to the optimization of reconfigurable millimeter-wave passive reflectors. In the proposed formulation, the incident-wave frequency is treated as a generalized cost parameter, consistently with the broader interpretation introduced in [13]. The term *generalized cost parameter* does not imply an economic, computational, or energetic cost; rather, it denotes an external parameter that defines a family of related multi-objective optimization problems. In the present application, each value of the incident-wave frequency defines a distinct Pareto optimization problem.

For each frequency, two competing objectives are considered: the negative radar cross section (RCS), −RCS, and the physical surface area of the antenna array. RCS maximization is therefore formulated as the minimization of −RCS, while the physical surface area is minimized directly. The corresponding utopia point is determined independently for each frequency, and the Pareto-optimal configuration having the minimum Euclidean distance from the corresponding utopia point is selected as the best-compromise solution. The collection of these best-compromise configurations over the considered frequency range defines the Pareto meta-front for the electromagnetic problem investigated in this paper.

This formulation is particularly suitable for broadband electromagnetic design because it provides information that cannot be obtained from an individual Pareto front alone. While each conventional Pareto front describes the trade-off between electromagnetic performance and physical size at a fixed frequency, the Pareto meta-front tracks the evolution of the best compromise as the operating frequency changes. It therefore provides a systematic means of identifying configurations that offer a favorable balance between electromagnetic performance and physical dimensions throughout a prescribed frequency range.

As a case study, the proposed methodology is applied to the design of a linear reconfigurable passive reflector intended for intelligent reflecting surface applications. The proposed array consists of dipole elements with variable geometrical parameters and reactive loads connected to the individual element ports. Reconfigurability is achieved by dynamically switching the reactive loads, thereby modifying the phase response of the individual elements and controlling the phase distribution across the array. This enables electronic steering of the reflected beam without requiring active amplification.

The optimization is performed over the 50–70 GHz millimeter-wave frequency range. At each frequency, the negative RCS and the physical surface area of the reflector are considered as competing objectives, and the corresponding best-compromise configuration is identified through its Euclidean distance from the utopia point. The resulting family of best-compromise configurations is then used to construct the Pareto meta-front, providing a systematic description of the trade-off between electromagnetic performance and physical dimensions throughout the operating frequency range.

The main contribution of this paper is the extension of the Pareto meta-front methodology to reconfigurable electromagnetic devices, with specific application to passive millimeter-wave reflectors for intelligent reflecting surface applications. The proposed approach provides a systematic alternative to selecting a single design through arbitrary objective-weighting factors and allows the best compromise between electromagnetic performance and physical array size to be tracked as a function of frequency.

2. Array design

A reflectarray architecture, incorporating dipole elements which are specifically designed without a contiguous ground plane, is considered. This configuration is intentionally chosen to minimize significant signal attenuation at frequencies outside the operational band, ensuring that the reflectarray's presence does not degrade the transmission performance of co-existing systems operating in other frequency ranges, below the considered high-frequency band (for instance 0.9 GHz, 1.8 GHz).

The final, complete reflectarray design will encompass a substantial number of elements, necessitating significant computational resources for comprehensive full-array electromagnetic simulation. To mitigate this excessive calculation burden and improve computational efficiency, a sub-array analysis methodology is employed [14, 15]. This technique facilitates faster processing by decomposing the large antenna array into smaller, more computationally manageable groups for independent analysis. By accurately analyzing the performance of these individual sub-arrays, this modular approach enables more accurate predictions of the full array's overall performance characteristics, including its radiation patterns and gain. Furthermore, this modularity inherently simplifies fault diagnosis, streamlining the process of localizing and resolving potential issues within a specific section of the array. In the present study, the sub-array is defined as a linear array consisting of 15 vertically oriented dipole antennas, as depicted in Fig. 2.

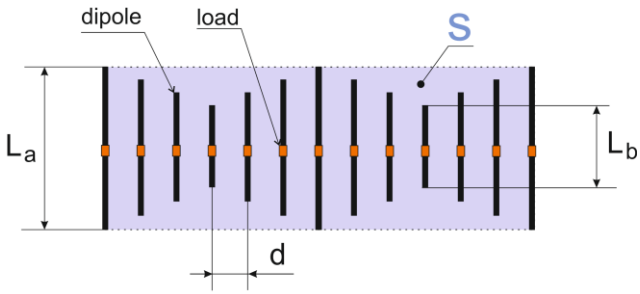
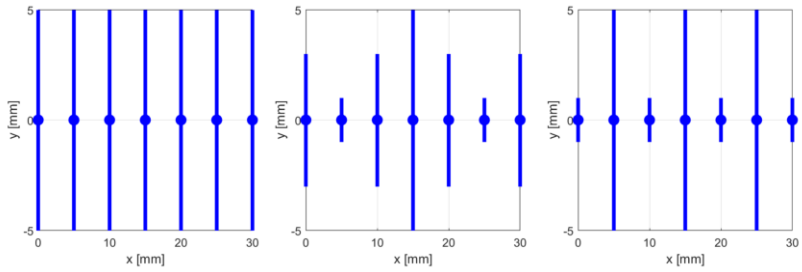


Fig. 2. The geometry of the dipole array

To achieve multiband operation, the array is synthesized using dipoles of varying lengths. The specific distribution of the dipole lengths is governed by the parameter L_f which controls the length on n dipole element $L(n)$. The length on n dipole element $L(n)$ is defined by (1):

$$L(n) = \left| (L_a - L_b) \cdot \left(\cos\left(n \cdot \frac{\pi}{2} \cdot L_f \right) \right)^2 + L_b \right|. \tag{1}$$

In (1), L_a denotes the length of the longest dipole, whereas L_b denotes the length of the shortest element. The parameter L_f controls the dipole-length distribution along the array. Figure 3 presents different dipole-length distributions corresponding to selected values of L_f. In the proposed formulation, L_f varies from 0 to 1 according to a sinusoidal profile. For clarity, only seven array elements are shown in Fig. 3, $(1 < n < 7)$. In this example, the length of the longest dipole is $L_a = 10$ mm, the length of the shortest dipole is $L_b = 2$ mm, and the element spacing is $d = 5$ mm. Three representative array geometries are presented for $L_f = 0$, $L_f = 0.5$ and $L_f = 1$.



(a) (b) (c)

Fig. 3. The dipole length distribution corresponding to different L_f parameters: (a) $L_f = 0$; (b) $L_F = 0.5$; (c) $L_f = 1$

3. Array optimization methodology

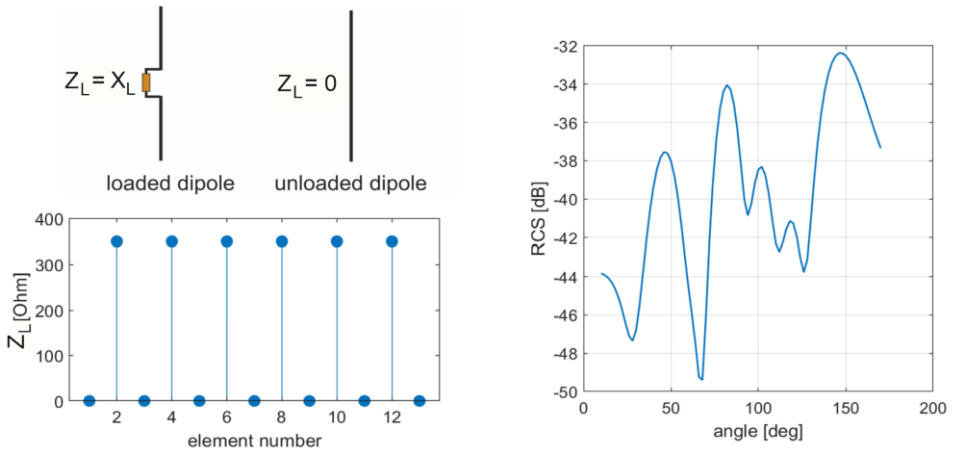
The primary objective of the optimization process is to maximize the reflected energy while simultaneously minimizing the physical surface area of the antenna array. The reflected energy is quantified using the Radar Cross Section (RCS), a standard metric in electromagnetic analysis. Specifically, this study employs the concept of the bistatic RCS, which measures the amount of energy scattered by a target in the direction of a receiver, given that the transmitter and receiver are spatially separated. The bistatic RCS is defined as the equivalent area of the target (here the dipole array) that intercepts the incident power and, if that power were re-radiated isotropically, would produce the same received power at the receiver. Crucially, unlike the monostatic RCS (where the transmitter and receiver are co-located), the bistatic RCS is a function of the specific scattering direction.

The optimization is formulated as a minimization problem with a multi-objective function composed of two principal components: f_1 (2) which relates to the negative of the RCS (to convert maximization to minimization), and f_2 (3), which represents the physical surface area of the array. The minimization of the array surface results from the need of increasing effectiveness of the reflector. In fact, the desired structure will have good reflection performance (possibly high RCS) with small physical dimensions. In such case the overall performance of array consisting of optimized subarrays would be also increased. The performance is further evaluated as a function of the incidence angle, denoted as $\varphi_{i1,i2}$, in the x-y plane. For simplicity and to establish a manageable initial design space, the optimization considered only two specific incidence angles: $\varphi_{i1,i1} = 40°$ and $\varphi_{i1,i2} = 60°$.

$$f_1 = -\min_{\varphi_{i1,i1},\varphi_{i1,i2}} \left(\max_{X} (\mathrm{RCS}) \right), \tag{2}$$

$$f_2 = (n-1) \cdot d \cdot L_a. \tag{3}$$

The proposed reflectarray achieves beam steering using switchable reactive impedances (X), which are selectively connected to the dipole elements according to the required beamforming state. As illustrated in Fig. 4, a specific impedance configuration defines the switch states shown in Fig. 4(a), while the corresponding Radar Cross Section (RCS) in the horizontal plane is presented in Fig. 4(b).



(a) (b)

Fig. 4. The example of the dipole array beam steering by employing a set of switchable impedances X: (a) state of switches; (b) resulting RCS as the function of angle in horizontal plane

The range of reactance variations is from 0 Ω to 500 Ω. By selectively connecting or disconnecting the impedances at each dipole, a precise phase shift of the reflected wave is introduced, which consequently redirects the main beam towards a desired angle.

Because each switching configuration requires a separate full-wave electromagnetic analysis, an exhaustive evaluation of all $2^{15} = 32\,768$ binary states of the 15-element array would be computationally prohibitive. The number of switching states was therefore limited to a deterministic codebook of 11 configurations. This reduction was particularly important because, at each iteration of the optimization algorithm and for a given frequency value, every candidate design was analyzed for two directions of wave incidence, $\varphi_{i1} = 40^\circ$ and $\varphi_{i2} = 60^\circ$. Consequently, evaluating the adopted codebook required $2 \times 11 = 22$ electromagnetic simulations for each candidate design and operating frequency. Specifically, the switching configurations were generated using the control parameter $e_s \in \{0, 0.1, \ldots, 1.0\}$. For a given value of e_s, the state of the switch connected to the n-th dipole, where $n = 1, \ldots, 15$, was determined as

$$s_n(e_x) = \frac{1}{2}\left[1 + \operatorname{sgn}\left(\cos\left(\pi e_x n\right)\right)\right], \quad n = 1, \ldots, 15, \tag{4}$$

where $(s_n = 0)$ and $(s_n = 1)$ represent the disconnected and connected states, respectively. Assigned a value of e_s, a complete 15-bit switching vector was then generated. For each incidence direction angle, the RCS was subsequently calculated for all the 11 switching configurations, and the highest value obtained from this set was used to compute the maximum-RCS envelope. The same codebook and simulation procedure were consistently applied throughout the whole optimization procedure. This simplifying assumption substantially reduced the computational time, without altering the formulation of the optimization methodology, although the resulting RCS envelope represents the best performance within the adopted codebook rather than the global maximum over all possible switching states. For the sake of an example, 3 combinations of switching states for e_s values 0, 0.5 and 1 is presented in Fig. 5.

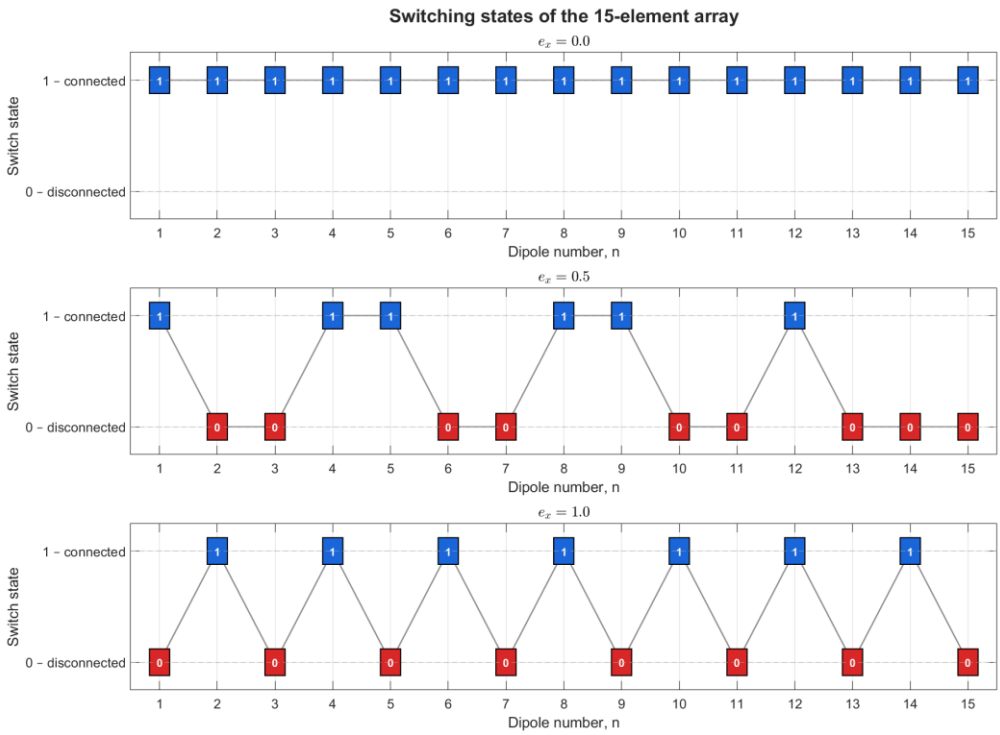


Fig. 5. The example of 3 combinations of switching states for e_s values 0, 0.5 and 1, respectively

Eventually, the RCS was evaluated across 11 distinct combinations of impedance switching states. These combinations ranged from the state where all impedances were disconnected (the base case) to the case where all impedances were connected, including alternating connection patterns (e.g., connected/disconnected at successive elements). Each unique switching configuration yielded a different RCS performance. Given that such switching activity is analogous to the mechanism by which the steering algorithm would dynamically operate (beamformer), we tested all these combinations and defined the maximum RCS values across all states as the envelope, as illustrated in Fig. 6. For each frequency and for the evaluation of f_1, the envelope is based on the set of 11 switching configurations. In turn for each switching configuration the RCS has to be evaluated for φ_{i1} angle ranging from 90° to 180° with the step of 5°.

The objective function component f_1 is designed to maximize the minimum value of this envelope, ensuring a robust and high reflection efficiency across all operational steering states.

All in one, the optimization problem reads: *considering the design vector* d, L_a, L_b), *find the family of Pareto fronts indexed by frequency f that simultaneously minimizes* (1) *and* (2) *against a set of switchable impedances X.*

Upper and lower bounds of design variables are assigned in Table 1.

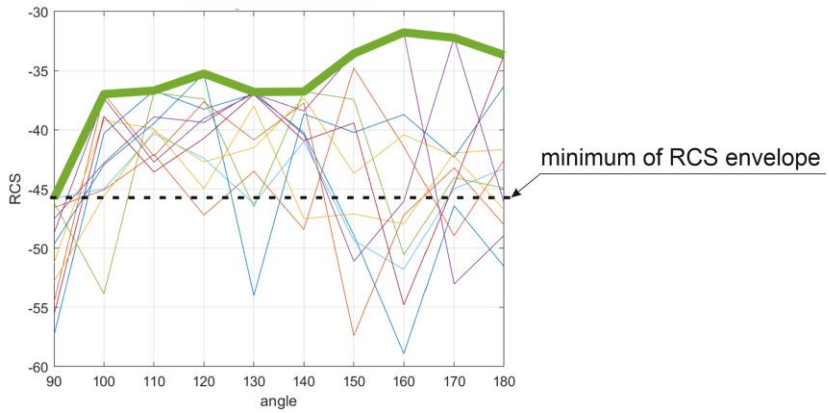


Fig. 6. Example of RCS values for all considered states of impedance switches and performance envelope

Table 1. Upper and lower bounds of design variables

Design variable	Lower bound	Upper bound
X [Ω]	0	500
L_f	0	1
d [mm]	1	50
L_a [mm]	1	10
L_b [mm]	1	10

In the multi-objective optimization problem considered here, the operating frequency serves as an indexing parameter for which the goal is to determine a locus of meta-optimal solution points, each belonging to the corresponding Pareto front for that specific frequency. The term meta-optimal point is used to designate a Utopia-like solution for the given frequency, representing the best achievable trade-off between the competing objectives. A key aspect is to investigate the relationship and consistency among these Utopia-like solutions across the range of different frequencies, as schematically illustrated in Fig. 7. Similar approach was used in [13] with an application to electromechanics.

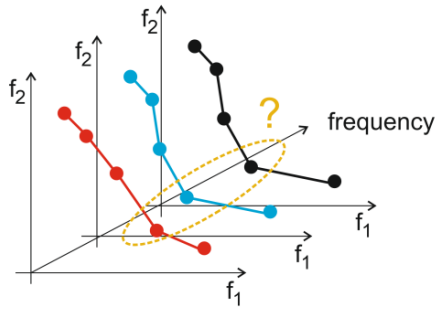


Fig. 7. Concept of meta-optimal points

The optimization was carried out using the Non-dominated Sorting Genetic Algorithm – NSGA II, which is the one of the most widely adopted evolutionary algorithm for approximating the Pareto front in multi-objective problems [16]. The computational settings for the algorithm were established with a population size of 10 and a total number of 20 generations. To accurately evaluate the objective function (i.e., to calculate the RCS), a Method of Moments (MoM) solver for metal structures implemented in MATLAB was utilized [17]. This technique calculates the surface currents on the antenna structure by discretizing the metallic surface into a set of triangle patches. The direct problem solver, which provides the RCS evaluation required for the objective function, is based on a custom function implemented in MATLAB.

The optimization was performed at three representative frequencies (50, 60, and 70 GHz) due to the computational complexity of the electromagnetic analysis. In fact, since the employed Method of Moments (MoM) solver operates in the frequency domain, separate electromagnetic simulations are required for each frequency, incidence angle, and switching configuration. Furthermore, these simulations must be repeated for each candidate solution evaluated by the genetic algorithm. Consequently, increasing the number of analyzed frequencies would substantially increase the computational cost. The selected frequencies provide a representative demonstration of the proposed Pareto meta-front methodology, while denser frequency sampling and more complex reflectarray geometries remain subjects of future investigations.

4. Optimization results

The NSGA-II algorithm was applied to approximate the Pareto fronts across three distinct operating frequencies: 50, 60 and 70 GHz. In order to identify a robust, single best compromise solution that performs optimally across a multi-frequency domain, the analysis compares the distance to the Utopia point for individual solutions belonging to the different frequency-specific Pareto fronts. For this comparative analysis to be meaningful, the components of the objective function were first normalized. The ideal Utopia point – representing the theoretical optimum where both objective components are simultaneously minimized – was defined as the [–2–2] point in the normalized objective space.

The optimization results are processed in order to identify meta-optimal solutions using two complementary criteria: proximity to the Utopia point in the objective space and proximity in the design-variable space, respectively. The first criterion identifies the best trade-offs between reflected energy and surface area, although it may lead to different physical designs. The second criterion supports the selection of a common final geometry.

Figure 8 shows the solutions closest to the Utopia point, marked with “o”, for the tested frequencies of 50, 60, and 70 GHz. The relevant Pareto fronts may be non-convex, as observed for 60 GHz. The corresponding design variables are listed in Table 2.

Alternatively, robustness and manufacturability were prioritized by selecting solutions with the smallest distance in the design space, i.e., with the most similar design variables such as dipole lengths and spacing, regardless of the Utopia point. This approach identifies a common configuration that provides good performance across all operating frequencies while minimizing structural changes. These solutions are marked with “+” in Fig. 8, and their design parameters are listed in Table 3.

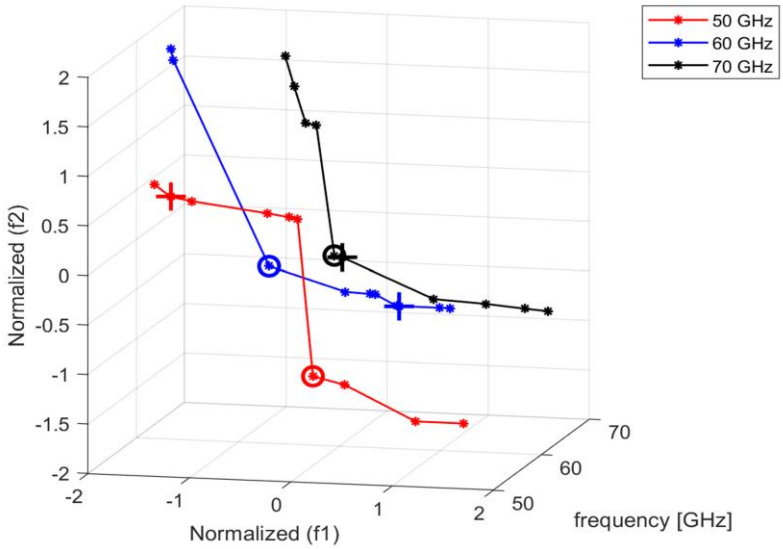


Fig. 8. Pareto fronts for 3 considered frequencies: the solutions located the closest to utopia in the objective space "o", the solutions located the closest to utopia in the design space "+"

Table 2. Design variables for the solutions located the closest to utopia in the objective space

Frequency [GHz]	**Design variables**				
	X [Ω]	L_f	d [mm]	L_a [mm]	L_b [mm]
50	169.5	0.151	3.3	3.6	2.5
60	341.9	0.60	1.6	5.5	6.7
70	200.7	0.443	1.6	5.0	5.9

Table 3. Design variables for the solutions that had the most similar values for the design variables

Frequency [GHz]	**Design variables**				
	X [Ω]	L_f	d [mm]	L_a [mm]	L_b [mm]
50	169.5	0.98	5.3	5.9	7.1
60	341.9	0.60	1.6	5.5	6.7
70	200.7	0.443	1.6	5.0	5.9

Comparing the results in Fig. 8 and Tables 1 and 3, the two selection criteria identify the same solution at 60 GHz and, separately, the same solution at 70 GHz. This agreement does not mean that the 60 and 70 GHz solutions are identical to each other; rather, it shows that the objective-space and design-space criteria converge to the same frequency-specific solution at each of these two frequencies. At 50 GHz, the solutions selected by the two criteria remain at the greater distance to each other in both the design and objective spaces, compared to 60 and 70 GHz.

5. Conclusions

This study introduced and applied an original multi-objective optimization framework for the design of broadband reconfigurable reflectarray antennas. Its main methodological contribution is the meta-optimal solution concept, which extends Pareto-like optimization by identifying robust designs across an indexed parameter space, here represented by operating frequency. By comparing the distance to the Utopia point for solutions obtained at 50, 60, and 70 GHz, the method revealed invariant properties in both the objective-function space and the physical design-parameter space.

The meta-optimal solution analysis also provided practical design guidance by enabling the identification of suitable inductive load values for the unit-cell elements, supporting broadband and steerable operation. By reducing the multi-frequency problem to a single compromise-selection framework, the proposed approach offers quantitative support for choosing optimal trade-off solutions under complex design constraints.

Although demonstrated for a linear dipole reflectarray, the methodology is general and can be applied to other antenna and electromagnetic structures involving coupled physical and electrical parameters. Future work will extend the approach to more advanced stacked-array architectures with dual-polarization capability, aiming to further improve system performance and flexibility.

References

[1] Nayeri P., Yang F., Elsherbeni A.Z., *Reflectarray Antennas: Theory, Designs, and Applications*, Wiley-IEEE Press, Hoboken, NJ, USA (2018).

[2] Hum S.V., Perruisseau-Carrier J., *Reconfigurable Reflectarrays and Array Lenses for Dynamic Antenna Beam Control: A Review*, IEEE Transactions on Antennas and Propagation, vol. 62, no. 1, pp. 183–198 (2014), DOI: 10.1109/TAP.2013.2287296.

[3] Khan A., Hassnain Mohsan S., Elfikky A., Boghdady A.I., Ahmad S., Innab N., *A survey of intelligent reflecting surfaces: Performance analysis, extensions, potential challenges, and open research issues*, Vehicular Communications, vol. 51 (2025).

[4] Alghamdi R. *et al*., *Intelligent Surfaces for 6G Wireless Networks: A Survey of Optimization and Performance Analysis Techniques*, IEEE Access, vol. 8, pp. 202795–202818 (2020).

[5] Katwe M. *et al*., *An Overview of Intelligent Meta-surfaces for 6G and Beyond: Opportunities, Trends, and Challenges*, IEEE Communications Standards Magazine, vol. 8, no. 4, pp. 62–69 (2024).

[6] Sohua I.A., *et al*., *Shaping the Future of Wireless Communication: An Analysis of Reflectarray Antennas for 5G/6G*, ASEAN Engineering Journal, vol. 15, no. 3, pp. 125–135 (2025), DOI: 10.11113/aej.v15.23195.

[7] Al-Safi J.K.S., Alsahlanee A.T.R., *6G Communication Systems Utilizing Intelligent Reflective Surfaces for Improved Data Rates Based on AI*, Computing and AI Connect, vol. 2, no. 24 (2025).

[8] Harrington R.F., *Reactively controlled directive arrays*, IEEE Transactions on Antennas and Propagation, vol. 26, no. 3, pp. 390–395 (1978), DOI: 10.1109/TAP.1978.1141852.

[9] Miettinen K., *Nonlinear Multiobjective Optimization*, Kluwer Academic Publishers (1999).

[10] Branke J., Deb K., Miettinen K., Słowiński R., *Multiobjective Optimization: Interactive and Evolutionary Approaches*, Springer (2008).

[11] Di Barba P., *Multi Objective Optimal Design in Electricity and Magnetism*, Springer (2010).

[12] Angiulli G., Versaci M., *Electromagnetic Characterization of Concrete by Jonscher Universal Dielectric Model: Numerical Validation of Different Nonlinear Optimization Algorithms*, IEEE Access, vol. 13, pp. 142635–142650 (2025), DOI: 10.1109/ACCESS.2025.3598642.

[13] Di Barba P., Galdi R., Mognaschi M.E., *Pareto Meta-Front for the Optimal Design of Reconfigurable Devices in Electromechanics*, Electronics Letters, vol. 61, no. 1 (2025), DOI: 10.1049/ell2.70489.

[14] Mukit N., Islam M.R., Habaebi M.H., Alam A.H.M.Z., Abdullah K., Malek N.F.A., Nibir R., Adnan N.H.M., Osman E., *Designing large-scale antenna array using sub-array*, Bulletin of Electrical Engineering and Informatics, vol. 8, no. 3, pp. 906–915 (2019).

[15] Boulos F., Caizzone S., Winterstein A., *A subarray-based antenna design for satellite communications ground terminals in Ka band*, Proceedings of the 26th Ka Broadband Communications Conference, pp. 1–9 (2021).

[16] Deb K., Pratap A., Agarwal S., Meyarivan T., *A fast and elitist multiobjective genetic algorithm: NSGA-II*, IEEE Transactions on Evolutionary Computation, vol. 6, no. 2, pp. 182–197 (2002), DOI: 10.1109/4235.996017.

[17] MathWorks, Inc. (2026), *MATLAB Antenna Toolbox Documentation: Method of Moments Solver for Metal and Dielectric Structures*, accessed August 2026.